Thermodynamics of the self-assembly of non-ionic chromonic molecules using atomistic simulations. The case of TP6EO2M in aqueous solution.

Anna Akinshina[a], Martin Walker[b], Mark R. Wilson[b], Gordon J. T. Tiddy[a], Andrew J. Masters[a], and

Paola Carbone[a]

[a] *School of Chemical Engineering & Analytical Science, The University of Manchester, Oxford Road, Manchester, M13 9PL*
[b] *Department of Chemistry, Durham University Science Laboratories, South Road, Durham DH1 3LE*

ABSTRACT

Atomistic molecular dynamic simulations have been performed for the non-ionic chromonic liquid crystal 2,3,6,7,10,11-hexa-(1,4,7-trioxa-octyl)-triphenylene (TP6EO2M) in aqueous solution. TP6EO2M molecules consist of a central poly-aromatic core (a triphenylene ring) functionalized by six hydrophilic ethyleneoxy (EO) chains, and have a strong tendency to aggregate face-to-face into stacks even in very dilute solution. We have studied self-assembly of the molecules in the low concentration range corresponding to an isotropic solution of aggregates, using two force fields GAFF and OPLS. Our results reveal that the GAFF force field, even though it was successfully used previously for modelling of ionic chromonics, overestimates the attraction of TP6EO2M molecules in water. This results in an aggregation free energy which is too high, a reduced hydration of EO chains and, therefore, molecular self-assembly into compact disordered clusters instead of stacks. In contrast, use of the OPLS force field, leads to self-assembly into ordered stacks in agreement with earlier experimental studies of triphenylene-based chromonics. The free energy of association follows a "quasi-isodesmic" pattern, where the binding free energy of two molecules to form a dimer is of the order of 3 RT larger than the corresponding energy of addition of a molecule into a stack. The obtained value for the binding free energy, $\Delta_{agg}G^0 = -12$ RT, is found to be in line with the published values for typical ionic chromonics (-7 to -12 RT), and agrees reasonably well with the experimental results for this system. The calculated interlayer distance between the molecules in a stack is 0.37 nm, which is at the top of the range found for typical chromonics (0.33-0.37 nm). We suggest that the relatively large layer spacing can be attributed to the repulsion between EO side chains.

1 Introduction

Chromonic mesogens are a non-conventional form of lyotropic liquid crystal molecule[1-4]. Typically, such molecules are composed of a hydrophobic disc (often formed from an extended aromatic region) surrounded by solubilising groups. This characteristic molecular structure leads to aggregation in aqueous solution, most usually into molecular stacks[5]. At higher concentrations stacks self-organise to form lyotropic mesophases. Aggregation occurs in the absence of a critical micelle concentration, and often at extremely low concentrations. There is considerable interest currently in chromonic systems as media for alignment of nanorods,[6] for thin film fabrication,[7] and for real-time microbial sensors.[8, 9]

Most well-studied chromonics molecules are ionic systems, composed of a large disc-shaped chromonic anion and a small cation. However, in principle it is possible to design non-ionic chromonic systems. Such systems open the possibility of using supramolecular interactions to design tailor made nanostructures in solution for deposition at surfaces, or for fabrication of new organic-inorganic composites from the chromonic mesophase by a sol-gel process.[10]

An early non-ionic chromonic mesogen 2,3,6,7,10,11-hexa-(1,4,7-trioxa-octyl)-triphenylene (TP6EO2M), was synthesized by Boden et al. in 1985.[11] TP6EO2M consisted of a triphenylene poly-aromatic core, made water soluble by the presence of six ethylene oxide chains on the periphery of the molecule (see Figure 1). This molecule was designed specifically to form only rod-shaped aggregates in aqueous solutions.[12, 13] The mesophases formed by TP6EO2M in water have been extensively studied using proton NMR[12-16], x-ray diffraction,[12, 13] and DSC[14] across a wide range of concentrations and temperatures. In solution the molecules aggregate into small randomly-oriented stacks which, depending on temperature and concentration, self-organize into a variety of ordered phases. Among these are mixed isotropic phase, nematic phase, columnar hexagonal phase and mixed columnar and crystal phases.[11-13, 17] The aggregation process is thought to be isodesmic, implying that the addition of a molecule to a stack is associated with the same increment of free energy, regardless of the stack size.[1-4, 16] The molecule TP6EO2M is remarkable because it has the optimal balance of hydrophobic and hydrophilic interactions to exhibit chromonic behaviour. The compound with one less EO unit in each side chain, TP6EO1M, was found to be sparingly soluble in water and, conversely, the compound with one more EO unit in each chain, TP6EO3M, is too hydrophilic and even though it aggregates in low concentrations, no ordered phases were observed above the freezing point.[12, 16]
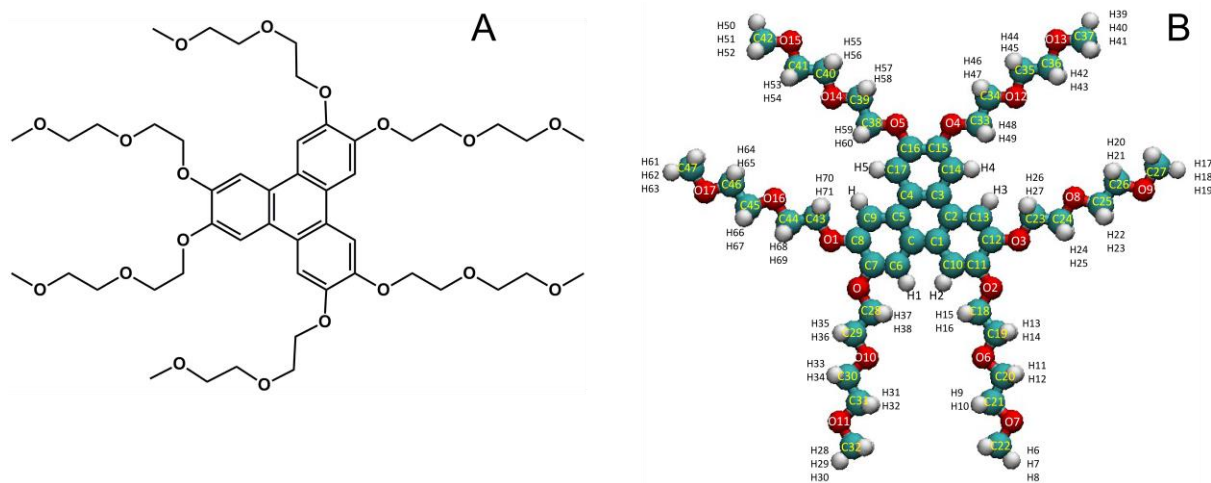
Several attempts have been made to study TP6EO2M molecules theoretically[18, 19] and by computer simulations.[20, 21] Taylor and Herzfeld[18] studied aggregation of polydisperse rigid spherocylindrical rods using scaled particle theory and obtained a temperature-concentration theoretical phase diagram in good qualitative agreement with the experimental one of Boden et al.[13] However, as the authors note, including aggregate flexibility would vastly improve the model. The issue of rod flexibility was later addressed by Hentschke et al. in their theoretical work.[19] Considering a system of monodisperse self-assembling rods described by a simple excluded volume model, the authors obtained persistence length-concentration phase diagram where experimental coexistence volume fractions follow very closely the isotropic/nematic (IN) coexistence line. As shown by van der Schoot,[22] the aggregate flexibility and polydispersity are both important model features to a proper description of the isotropic-nematic phase transition for such systems. Edwards et al.[20] performed Monte Carlo simulations of TP6EO2M molecules using a rudimentary disk-shaped model consisting of a central hydrophobic sphere surrounded by six, inplane, hydrophilic spheres. Attraction between molecules was modelled by a square well potential between the central (hydrophobic) spheres of

two molecules. At low concentrations the model molecules self-assembled into linear aggregates and with increasing concentration nematic and hexagonally packed columnar phases were observed.

The first atomistic molecular dynamic simulation of TP6EO2M molecules was performed by Bast and Hentschke.[21] A force field based on AMBER/OPLS parameters was applied to study a periodic stack of 8 molecules in SPC/E water. Various stack properties such as effective diameter of the stack, rotational diffusion of the molecules within the stack, distances between the neighbouring molecules, flexibility of the stack and monomer-monomer contact free energy gain were evaluated in this work. The values obtained for centre of mass and stacking distances (4.5 and 4.2 Å, respectively) agree well with the experimentally obtained ring-ring separation of 4 Å.[16] However, the result obtained for the monomer-monomer contact free energy (−27 to −44 RT) was considerably greater than the experimental finding (~ −14 RT).

In a recent publication, Chami and Wilson reported simulation results on the ionic chromonic dye, Sunset Yellow (Edicol, SSY) using the GAFF force field for the dye and TIP3P water model.[23] Here, a combination of long atomistic simulations and DFT calculations provide a detailed explanation for NMR shifts in solution; and the study is able to reproduce the molecular separation within stacks, the experimental association free energy and provide the first atomistic simulation of a chromonic nematic phase in water.

In this paper we present atomistic simulation studies for TP6EO2M in dilute aqueous solution. We present results obtained using two major force fields, GAFF and OPLS, and clearly demonstrate that for this type of non-ionic chromonic molecule the OPLS force field gives more reliable results. We additionally explore the association free energy, showing that we can reproduce the result obtained from fitting to experimental data, and demonstrating that association in TP6EO2M is more subtle than originally thought: association follows a "quasi-isodesmic" pattern with the binding free energy of two molecules to form a dimer ~ 3 RT larger than the corresponding free energy of addition of a molecule to a chromonic stack.

Figure 1. (A) The chemical structure and (B) the all-atom model of TP6EO2M used in this study. Colour code in (B): turquoise – carbons, red – oxygens, white – hydrogens. The numbers on the atoms are given for clarity, they correspond to those in the structure file and are referred in the text.

2 Methods

2.1 Force Fields

Molecular Dynamic simulations of chromonic molecules TP6EO2M in aqueous solution were carried out using the GROMACS 4.5.4 software package.[24, 25] The full atom model of the molecule is shown in Figure 1. We have performed simulations to compare the results of two force fields: GAFF and OPLS. The GAFF force field with modified electrostatics was successfully used previously by Chami and Wilson to study Sunset Yellow (SSY)[23], and this force field was therefore initially chosen to study our target TP6EO2M molecules. GAFF is compatible with the TIP3P water model, and this was used for the simulations here. The details of the GAFF parameters used are given in the Table I.

As it will be seen later, the GAFF simulation results differ significantly from experimental observations. Therefore, the OPLS-AA was used as an alternative force field. The bonded and nonbonded parameters for the carbon rings of the aromatic core were those used to model carbon nanotubes by Minoia et al.[26, 27] The parameters for the ethylene oxide (EO) chains were the standard OPLS-AA parameters already used in simulations of poly-ethylene oxide (PEO) chains in water.[28] Because TP6EO2M contains both, a poly-aromatic core and several EO chains, we consider OPLS as an appropriate choice. The OPLS force field parameters are given in the Table II. The OPLS-AA force field has been also used in a recent study of interactions between asphaltene molecules,[29] which have extended aromatic core (as in triphenylenes). Moreover, the OPLS-based force field has been used for simulations of a small stack of TP6EO2M previously.[21] The topology files for both force fields are available in the Supplementary material.

Tables I. The model parameters for GAFF force field.

Atom name	mass	charge	GAFF	
			σ (nm)	ε (kJ/mol)
ca (inner core C atoms C-C5)		−0.0100		
ca (core CH atoms C6 C9 C10 C13 C14 C17)	12.011	−0.1770	3.39967e-01	3.59824e-01
ca (outer core C atoms C7 C8 C11 C12 C15 C16)		0.1151		
ha (core H atoms H-H5)	1.0080	0.1420	2.59964e-01	6.27600e-02
os (near core atoms O-O5)		−0.3099		
os (middle atoms O6 O8 O10 O12 O14 O16)	16.000	−0.4306	3.00001e-01	7.11280e-01
os (periphery atoms O7 O9 O11 O13 O15 O17)		−0.4246		
s3 (CH2) C18 C23 C28 C33 C38 C43		0.1224		
C19 C24 C29 C34 C39 C44		0.1294		
C20 C25 C30 C35 C40 C45	12.011	0.1304	3.39967e-01	4.57730e-01
C21 C26 C31 C36 C41 C46		0.1244		
s3(CH3)		0.1187		
h1 (from core) H15 H16 H26 H27 H37 H38 H48 H49 H59 H60 H70 H71		0.0527		
H13 H14 H24 H25 H35 H36 H46 H47 H57 H58 H68 H69		0.0467		
H11 H12 H22 H23 H33 H34 H44 H45 H55 H56 H66 H67	1.0080	0.0437	2.47135e-01	6.56888e-02
H9 H10 H20 H21 H31 H32 H42 H43 H53 H54 H64 H65		0.0407		
h1 (CH3)		0.0207		

Tables II. The model parameters for OPLS force field.

Atom name	type	mass	charge	OPLS	
				σ (nm)	ε (kJ/mol)
CA (inner core C atoms C-C5)	opls_147		0.000		
CA (core CH atoms C6 C9 C10 C13 C14 C17)	opls_145	12.0110	−0.115	3.55e-01	2.9288e-01
CA (outer core C atoms C7 C8 C11 C12 C15 C16)	opls_727		0.200		
HA (core H atoms H-H5)	opls_146	1.00800	0.115	2.42e-01	1.2552e-01
OS	opls_180	15.9994	−0.400	2.90e-01	5.8576e-01
CT (CH2)	opls_182	12.0110	0.140	3.50e-01	2.76144e-01
CT (CH3)	opls_181		0.110		
HC	opls_185	1.00800	0.030	2.50e-01	1.2552e-01

2.2 Simulation details

For the self-assembly simulations the molecules were placed at random in a cubic simulation box and solvated with water. In all cases, the concentrations studied corresponded to the isotropic phase, as determined experimentally.[16, 17, 30] For both force fields, two systems were used at the same concentration of 8 wt% (8 TP6EO2M molecules with 4784 water molecules and 20 TP6EO2M molecules with 12048 waters), together with one system at an elevated concentration of 16 wt% (40 TP6EO2M molecules with 10720 waters).

The initial structures were subjected to initial energy minimisation step and a short constant-*NVT* ensemble simulation (500 ps) prior to long constant-*NpT* ensemble equilibration and production simulation runs. Constant-*NpT* equilibration runs were carried out for 100-200 ns to ensure that the simulation box was fully equilibrated and that all the molecules were self-assembled into aggregate(s), which were stable over time. The formation and stability of the formed aggregates was measured using cluster analysis (g_clustsize code) available with the GROMACS package. After the equilibration, the production runs were carried out at constant-*NpT* ensemble for 50 ns and the properties of the system were analysed. The simulations were carried out at a constant temperature of $T = 280$ K and a pressure of 1 bar with a time step of 2 fs. All bonds were constrained using the P-LINCS[31] algorithm. The neighbour list was updated every 5 steps. The same cut-off distance of 1.2 nm was applied to the neighbour list, Van der Waals and electrostatic interactions. The simulation temperature was controlled with a Nosé-Hoover thermostat[32, 33] with a time constant of 0.2 ps and the pressure controlled with an isotropic Parrinello-Rahman barostat[34, 35] with a time constant 5 ps and compressibility of $4.5×10^{-5}$ bar^{-1}. Electrostatics was calculated using the Particle Mesh Ewald (PME)[36, 37] algorithm.

3 Results and discussion

3.1 Self-assembly

Starting from randomly placed solute molecules, aggregation occurred rapidly for both the GAFF and OPLS models. The aggregation process, however, was different for the two force fields. Using GAFF, the molecules organised into a single unstructured aggregate (cluster) within the first 5 ns of the simulation time. Longer simulations showed only a slight compression of the aggregate cluster. After 20 ns the aggregate reached its final form and this structure remained unchanged for the rest of the simulation – a further 130 ns. Even though the cluster contained aligned molecules, in the form of dimers, trimers and tetramers, the shape of the cluster was oblate rather than the rod-like structure

expected for TP6EO2M molecules. Closer examination of the cluster, showed small stacks that were associated isotropically with either no water or only a few water molecules between them. This is illustrated in Figure 2(B-D).

In contrast, the OPLS force field gave results commensurate with previous studies.[12, 13, 17] The molecules organised themselves into dimers and trimers within the first 10 ns of the simulation; they formed two stacks of 2 and 6 molecules within 50 ns and a single stack containing all 8 molecules assembled after 90 ns. This 8-molecule stack remained stable for the rest of the simulation – a further 60 ns. The OPLS self-assembly process is illustrated in Figure 2(F-H).

The aggregation process and the stability of the aggregates formed were examined using cluster analysis. Two molecules were considered to be in a cluster if the distance between their centres of mass was less than r_{cut} = 0.9 nm (see Figure 4.1 in section 3.2). In Figure 2 (E) we show how the number of stacks (clusters) varies with simulation time for both GAFF and OPLS force fields. For both force fields the graphs show a sharp decrease in the number of clusters from an initial fully disperse system of 8 single molecules followed by a gradual levelling off of the number of clusters. For the GAFF model the graph shows that there are 2 clusters formed after ~20 ns and this value remains more or less constant for the following 130 ns. The r_{cut} value of 0.9 nm accounts for molecules that are associated in a columnar aggregate, but not if the aggregation occurs side by side, hence only anisotropic clusters can be detected, providing a measure of the chromonic nature of the aggregate. For the OPLS model the levelling off is slower, showing gradual assembling of the molecules into several small stacks first and then formation of a single stack after 90 ns.

The aggregation process observed with the OPLS model appears to be similar to those presented by Chami and Wilson for SSY chromonics.[23] SSY molecules quickly form small clusters, which organize into two tetramers after first 22 ns, followed by the merging of the tetramers into a single stack after 200 ns of the simulation time.
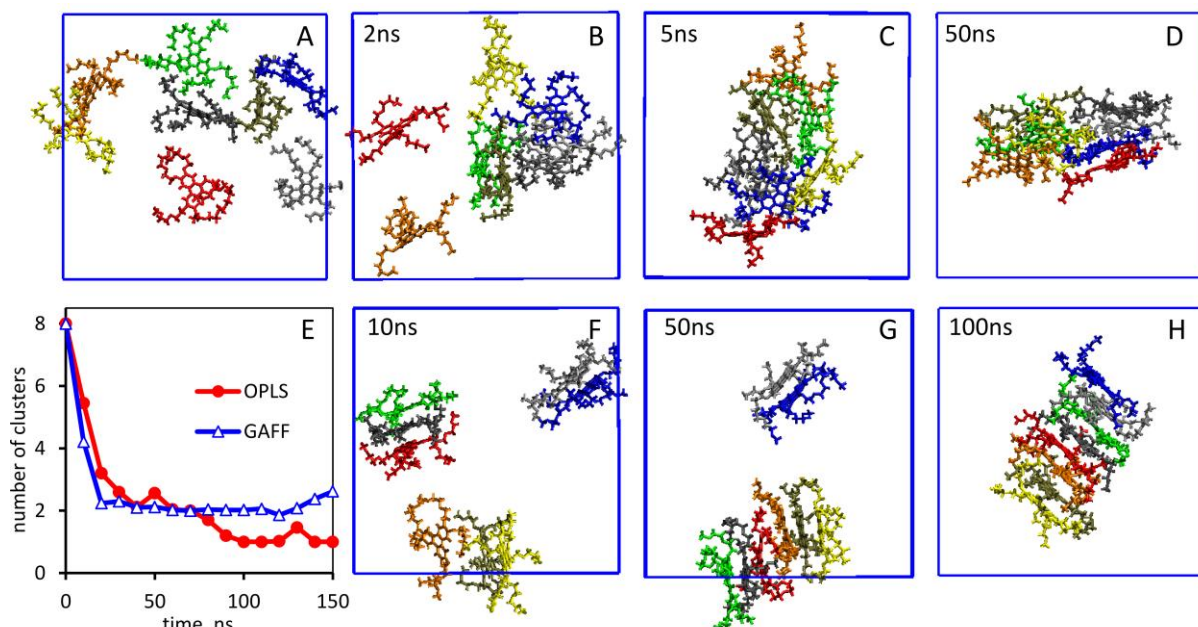

Figure 2. Self-assembly dynamics for 8 TP6EO2M molecules (8 wt%) with GAFF and OPLS force fields. (A) Starting configuration with randomly placed molecules (same for both force fields (B)-(D) GAFF force field, configurations for 2, 5 and 50 ns. (F)-(H) OPLS force field, configurations for 10, 50 and 100 ns. Molecules are coloured differently for better visibility. (E) Number of molecules in clusters plotted against simulation time, each point represents an average over 10 ns (blue, triangles – GAFF; red, circles – OPLS). The images were obtained using the VMD software package.[38]

The self-assembly process for the larger systems (both 20 molecules at 8 wt% and 40 molecules at 16 wt%) were found to be similar to those for the small system, but required longer simulation to reach equilibrium. The OPLS force field applied to a system of 20 random molecules formed a single stack after ~200 ns (Figure 3A), which remained stable over next 50 ns of simulation. The GAFF simulations produced an extended structure consisting of several small stacks associated at an angle to each other (Figure 3B). This structure, formed after the first 15 ns of simulation, does not measurably evolve with extended simulation times.

In the more concentrated system with OPLS model after 250 ns of simulation 40 molecules arrange into several stacks (one long and several short ones) randomly oriented (Figure 3D). The stacks do not associate to form a single cluster – they are stable, dissolved in water with the EO chains well solvated. In this case the molecules would not form a single stack just because the box size is too small for that, but the observed behaviour aligns well with the experimental observations. At the concentration studied, the solution of is known to be isotropic, implying that the formed stacks are polydisperse in size and oriented randomly in the solution.

The GAFF potential applied for the same system of 40 TP6EO2M molecules leads, once again, to a formation of a single compact aggregate (Figure 3C) and it is clearly observable that the system moves towards phase separation. Such behaviour contradicts the experimental observation as these molecules are soluble in water.[12, 16] Therefore, we suggest that the GAFF force field poorly describes this type of system. For TP6EO2M in water, our results show that GAFF potential leads to either, too strong attraction between the chromonic molecules, favouring phase separation over an aligned aggregate, or too weak attraction between EO chains and water, making the molecules hardly soluble. It is likely that a combination of these two effects leads to the resultant (disordered) cluster.

On the contrary, OPLS potential performs considerably better for TP6EO2M molecules. The self-assembly process results in a single or multiple soluble stacks, depending on the concentration, in agreement with the experimental predictions.[12, 13, 17]
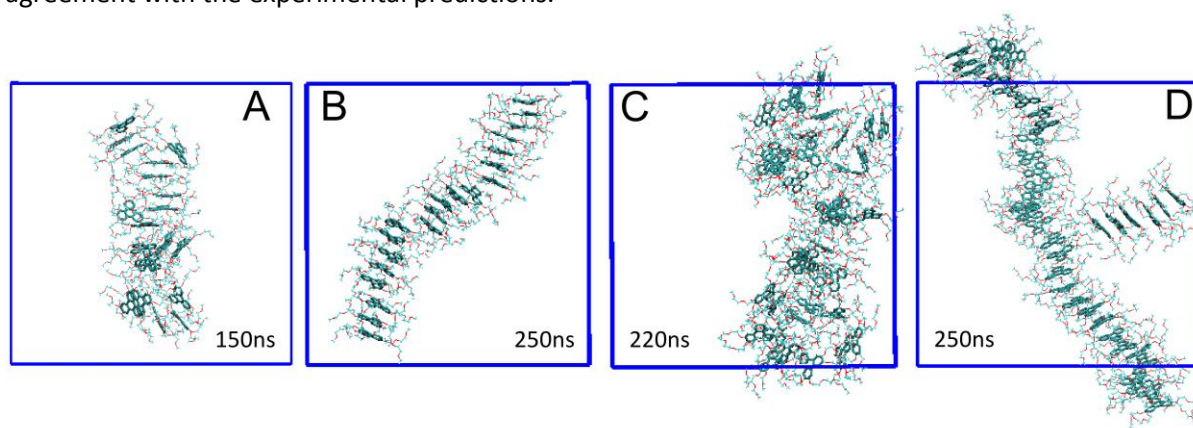
Figure 3. Final configurations for self-assembly of 20 and 40 TP6EO2M molecules (8 and 16 wt%) with GAFF and OPLS force fields. (A) 20 TP6EO2M molecules, GAFF; (B) 20 TP6EO2M, OPLS; (C) 40 TP6EO2M, GAFF; (D) 40 TP6EO2M, OPLS. The central aromatic cores are highlighted bold for better visualisation.

3.2 Distance between the molecules in the stack

Structural analysis was performed on the stack of 8 molecules obtained using the OPLS force-field. This system was used to study the separation between the neighbouring molecules within the stack. We consider two types of distances: an intermolecular distance, d_c, defined by the distance between the centre of mass of two neighbour molecules and an interlayer or stacking distance, d_s, defined by

the vertical distance between the two molecules (see Figure 4B). The stacking distance d_S was calculated as a projection of centre of mass distance, d_C, to the average vector of the normals to the aromatic cores for two adjacent molecules. Similar definitions were previously used in the TP6EO2M simulation work by Bast and Hentschke.[21]

The probability distribution functions for d_C and d_s are given in Figure 4A. The distribution curve for the stacking distance ranges between 0.3 and 0.5 nm with a sharp peak at 0.36 nm and the average value d_S = 0.37 ± 0.01 nm. Most of the values lie between 0.3 and 0.4 nm and a small tail stretches up to 0.5 nm. The distribution for the centre of mass distance, d_C, is wider and has a long tail at larger separations (up to $r \approx 1$ nm). Due to the long tail, the average centre of mass distance is larger, d_C = 0.46 ± 0.03 nm. However, the location of the maximum of the distribution is shifted only a little, to 0.37 nm. The fact that the maximum in d_C is slightly shifted to larger separations implies that the molecules in the stack are slightly offset.

The appearance of the tails at larger separations for both d_S and d_C is an indication of a bend in the stack. The distance between two molecules that are not parallel would be larger than that for the aligned molecules. This is schematically illustrated in Figure 4C. The time evolution of the intermolecular and stacking distances between two neighbouring molecules obtained for the last 50 ns of simulation are given in Figures 4 (D and E). Both graphs show that for one molecular pair the distance is larger than that for the other six pairs (orange curve) for the majority of the time. Such fluctuations in the stack structure are also observed in larger stacks of 20 molecules, both self-assembled from the solution and stacks that are pre-assembled. In nematic and columnar phases, where the stacks are well packed, we expect stacks to be slightly stiffer.

The obtained results for the stacking distance appear to be at the top of the range of 0.33-0.37 nm observed for typical chromonic systems.[3, 4, 23, 39, 40] In the simulations, the EO groups cause the molecules to lie at a slightly larger distance apart than would be preferred for the pure aromatic stacking. Two literature values have been reported for TP6EO2M. A value of d_S = 0.352 nm was obtained by Boden et al.[12] using X-ray diffraction, and a larger value of d_S = 0.4 nm was obtained by the same group 10 years later from measurements of proton NMR chemical shifts at T = 288 K.[16] Interestingly, the larger value was obtained in isotropic solution and the smaller value in the higher concentration columnar phase. One reason for the discrepancy in the reported experimental values could lie in molecules being more strongly held in stacks within the more concentrated phase, as seen in mesophase simulations of Chami and Wilson for sunset yellow. In the only published simulation work for TP6EO2M molecules by Bast and Hentschke,[21] the values for d_S and d_C were found to be 0.42 and 0.45 nm respectively, higher than both our results and experiment.
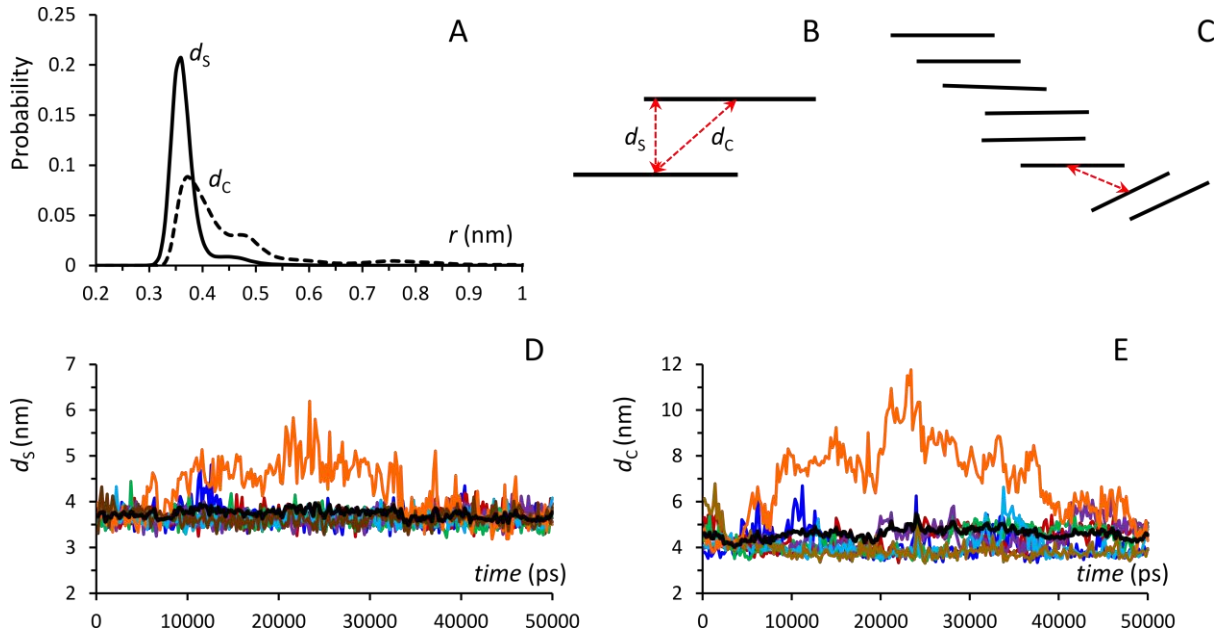
Figure 4. (A) Intermolecular (d_C) and stacking (d_S) distances between TP6EO2M molecules in a stack of 8 molecules. (B) Schematic illustration showing how the distances, d_C and d_S, are defined. (C) Schematic illustration of stack bend. (D) Stacking distance d_C as a function of time. (E) Intermolecular distance d_S as a function of time. In the graphs (D) and (E) distances between different dimers are shown with different colour and the black thick line shows the average value for d_S and d_C for all 7 dimers.

3.3. Free energy of association.

The free energy of association for two molecules was evaluated from the potential of mean force (PMF) profile along the separation distance between the centres of mass (COMs) of their aromatic cores using a set of constraint distance simulations. For each constraint distance between the two COMs the average constraint force was evaluated and the PMF was calculated by integrating the mean constraint force over the separation distance, using the following equation:[41-43]

$$V_{\text{PMF}}(r) = \int_{r_{\text{max}}}^{r_0} \left[\langle f_C \rangle_s + \frac{2k_{\text{B}}T}{s} \right] ds + C. \tag{1}$$

Here $\langle f_C \rangle$ is the averaged constraint force between the two COMs, k_{B} is the Boltzmann constant and T is the temperature. The second term in the integral, $2k_{\text{B}}T/s$, is the kinetic entropy term, arising from the fact that, when the direction between the molecules is not fixed, the free rotation of the molecules causes a larger volume to be sampled at larger separations. The integration is performed from r_{max}, where the molecules are not interacting to r_0, the smallest distance between the molecules. The simulations were carried out using the pull code implemented in the GROMACS package. To generate initial configurations with constrained distances between the COMs a system of two non-constrained molecules solvated in water was first equilibrated for 20 ns, then the COM of one molecule was pulled with respect to the COM of the second molecule with a pull rate of 0.01 nm ps^{-1}. For each chosen distance between COMs the system was again equilibrated for 10 ns and then simulated for a further 50 ns with a time step of 2 fs. During the production MD-run the forces were stored every 10 steps (0.02 ps), resulting in a total of 2.5 x 10^6 force values used for averaging. The errors for forces were calculated using a block average and the corresponding errors for PMF were calculated via the propagation rule. All the calculations were carried out in the constant-NpT ensemble with the same parameters used for self-assembly simulations. The distance between COMs was varied from r_0 = 0.3 to r_{max} = 2.4 nm where the spacing between neighbouring points

varied between 0.01 to 0.2 nm. The smaller spacing was used for the separations near the minimum. To calculate the free energy of association of a molecule with a small stack (dimer and trimer) the simulations were carried out in a similar way, but in these cases the distance between the COM of the aromatic core of a single molecule and a COM of a stack was constrained. Therefore, the minimum in the free energy profile for binding of a molecule to a stack become shifted to larger separations.

The profiles for potential of mean force (PMF) for two TP6EO2M molecules are presented for the two force fields, GAFF and OPLS, in Figure 5A. We define ΔG as the difference between the minimum value of $V_{PMF}(r)$ and the value at larger separations where $V_{PMF}(r)$ reaches a plateau. For the two force fields considered, the values obtained for the dimerization free energy were ΔG_{GAFF} = −51.8 ± 1.5 kJ/mol (−22.3 ± 0.6 RT) and ΔG_{OPLS} = −40.7 ± 1.4 kJ/mol (−17.5 ± 0.6 RT). The ΔG value obtained using the GAFF force field is 5 RT higher than the corresponding result for the OPLS force field. The stronger attraction between the molecules with the GAFF force field leads to the self-assembly of molecules into the more compact aggregates rather than ordered stacks.

If one were to assume that the distance between two molecules in dimer was fixed at the minimum of the PMF, r_{min}, then ΔG would correspond to the excess Gibbs energy of dimerization. Clearly, though, this is an over-simplification as dimers self-assembled in solution are not rigid structures. To take into account the fact that molecules in an unconstrained aggregate are exploring a range of separations, we make use of Wertheim's formalism for aggregating fluids.[44-47] This approach allows the shape of the whole PMF profile to be taken into account. We divide the PMF into a reference, short-range repulsive potential, u_{rep}, and a long range attractive potential, u_{att}, which is responsible for aggregate formation. This decomposition is somewhat arbitrary, but it turns out that the final results are extremely insensitive to how this split is made. We choose to use the Weeks-Chandler-Andersen approach[48], in which

$$u_{rep}(r) = \begin{cases} V_{PMF}(r) + \varepsilon & r < r_{min} \\ 0 & r > r_{min} \end{cases}$$

(2)

$$u_{att}(r) = \begin{cases} -\varepsilon & r < r_{min} \\ V_{PMF}(r) & r > r_{min} \end{cases}$$

Here ε is the negative of the minimum value of $V_{PMF}(r)$. This particular split is widely used in liquid state perturbation theory (see e.g. Hansen and McDonald[49]).

We then calculate the quantity Δ, given by

$$\Delta = 4\pi \int_0^\infty \exp(-\beta u_{rep}(r)) \left[\exp(-\beta u_{att}(r)) - 1 \right] r^2 dr$$

(3)

where β has its usual meaning of $1/k_B T$, where k_B is Boltzmann's constant and T is temperature. This has dimensions of volume and plays the role of an equilibrium constant. Thus if dimers and monomers were in equilibrium, with number densities ρ_2 and ρ_1 respectively, then

$$\Delta = \frac{\rho_2}{\rho_1^2}$$

(4)

Should we wish to work in terms of molar concentrations, rather than number densities, then the equilibrium constant for dimerization, K_{dim}, is given by

$$K_{\text{dim}} = \Delta \times \frac{N_A}{V_0} \tag{5}$$

where N_A is the Avogadro constant and $V_0 = 1$ dm^3 mol^{-1}. The standard Gibbs energy of dimerization, ΔG^0_{dim}, is then given by

$$\Delta_{\text{dim}} G^0 = -RT \ln K_{\text{dim}} \tag{6}$$

where R is the gas constant. Applying this approach we find $\Delta_{\text{dim}} G^0 = -14.7 \pm 0.6$ RT for the OPLS potential and $\Delta_{\text{dim}} G^0 = -19.8 \pm 0.6$ RT for the GAFF.

For the OPLS force field the value obtained for $\Delta_{\text{dim}} G^0 = -14.7$ RT appears to be somewhat larger than the reported values for stacking free energy for many other chromonics, which tend to be in the range of -7 to -12 RT.[5, 23, 39] For Sunset Yellow (SSY) and disodium cromoglycate (DSCG) the stacking free energy is about -7 RT[5, 23], for benzopurpurin 4B (Direct Red 2) it was found to be -10.2 RT[39] and -12 RT for the dye Blue 27[5]. A collection of free energy values for several chromonic dyes is given by Dickinson et al. in their chromonics review.[5] Observing the structure of the above dyes, one can notice that the larger the aromatic core, the higher the stacking free energy. In TP6EO2M molecules the core area is relatively large and the presence of EO chains, which are absent in the other dyes, may also play an important role. Experimental values for the stacking free energy of TP6EO2M can be found in the PhD thesis of J. Hubbard,[16] and are in the order of -14 RT at $T = 280$ K and mole fractions of $4.8 \times 10^{-5} - 24 \times 10^{-5}$ (0.25 -1.2 wt %).

However, these results for the stacking free energy are calculated by fitting of NMR chemical shifts in dilute solution. The latter are obtained as a mean over all stack sizes present in the concentration range, i.e. not just for two molecules, and it is known from the literature, that the dimerization free energy is usually higher than the binding free energy for larger stacks.[4] To examine the influence of larger aggregates, we calculated the free energy of binding of a molecule to a small stack of two and three molecules. The profiles of the binding free energy for two molecules, a molecule and a dimer and a molecule and a trimer for OPLS force field are presented in Figure 5B.
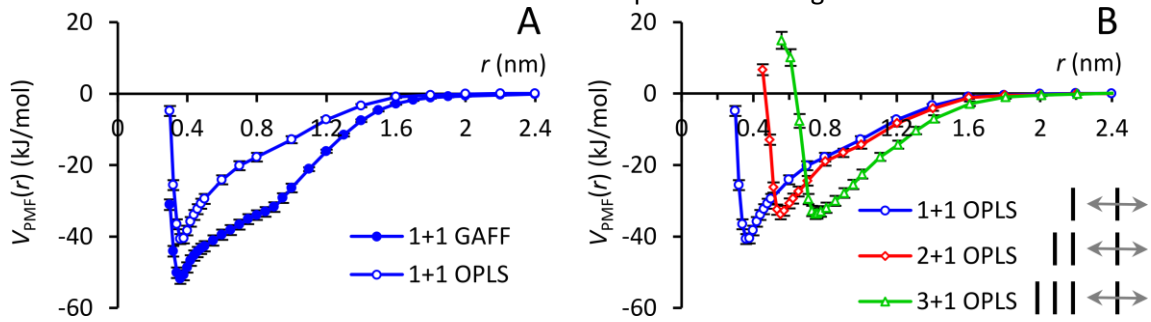
Figure 5. Free energy of association (PMF). (A) PMF for two molecules (1+1) for both force fields; (B) PMF for 1+1, 2+1 and 3+1 molecules for OPLS force field.

These calculations yield two significant results: (i) the free energy for binding of a molecule to a stack is smaller than the dimerization free energy and (ii) the ΔG values for binding of a molecule to a stack of two and three molecules are practically the same: implying larger aggregates will follow this regime.

Measuring the Gibbs energy change in terms of the depth of the minimum, binding a molecule to a dimer corresponds to $\Delta G = -33.8 \pm 1.4$ kJ/mol (14.5 $\pm$ 0.6 RT) while binding to a trimer corresponds

to $\Delta G = -33.6 \pm 1.5$ kJ/mol (14.4 ± 0.6 RT). Using the Wertheim approach, the standard Gibbs energy change for binding of a molecule to a dimer and a trimer is $\Delta_{agg}G^0 = -11.9 \pm 0.6$ RT and -12.4 ± 0.6 RT, respectively. These results are in physically meaningful agreement with the Hubbard's NMR data for these molecules.[16]

A slight difference between the free energy of dimerization and the free energy of addition of a molecule to a stack has been noted in other studies, and is discussed by Lydon in his review.[4] Chami and Wilson in their modelling study of Sunset Yellow dye found a dimerization free energy of ~−2 kJ mol^{-1} (−0.8 RT) higher than the free energy of binding the molecule to a stack.[23] Another example where the dimerization free energy is found to be slightly higher than the free energies for larger stacks is the work by Thuresson et al., where the interaction between clay platelets was studied.[50] However, in the latter study an implicit solvent model was used, so the difference between the free energies is attributed only to the free energy of the ions.

The results here suggest that the association in dilute solutions of TP6EO2M will follow a "quasi-isodesmic" pattern, and therefore differ slightly from the exponential distribution of aggregate sizes expected from a pure isodesmic association through a lower than expected number of monomers in solution. This was seen in the recent dissipative particle dynamics model of a non-ionic system by Walker et al.,[51] where, for large system sizes it was possible to directly measure aggregate distributions and hence deduce a free energy for each association step. It was again found that the free energy change of adding a monomer to a monomer differed from that of adding a monomer to a stack. This difference was attributed purely to entropic effects.

For many ionic chromonic systems, it is expected that $\Delta_{agg}G^0$ values are dominated by enthalpic effects.[1-4] However, for the non-ionic chromonic system studied here, the facts that (i) the area of the hydrophobic aromatic core for TP6EO2M molecule is larger than many typical chromonics and (ii) the water is also slightly depleted from the area around EO chains (see section 3.5) may lead to stronger increase in entropy of the system upon aggregation and, therefore, a rather large value for the stacking free energy.

In the case of other (ionic) chromonics the entropic contribution comes only from the release of water and ions upon aggregation. In our case there are two contributions to the entropy of aggregation: from the release of water and from confinement of the EO chains. Release of water provides a contribution to the entropy, while the chains lose their entropy being trapped in a stack, so this term is negative. The degree of hydration of a molecule at the end of a stack is greater than that of a molecule in the interior (see section 3.4), so the hydration entropy effect is different for dimer formation as compared to the formation of larger stacks. This entropy loss due to the confinement of PEO chains is higher for those molecules which are inside the stack than for those at the stack ends. The combination of the two effects, (i) the smaller entropy gain due to water release (explaining small difference in $\Delta_{agg}G^0$ for SSY), and (ii) the larger entropy loss due to confinement of the chains, leads to smaller total entropy contribution for a stack than for a dimer.

3.4 Hydration of EO chains

In order to estimate the hydration of EO chains upon molecular aggregation, we calculated the number of water molecules found in a shell of a radius of 0.3 nm around each of the EO group. The TP6EO2M EO oxygen atoms were selected as the binding target. Because we expect that the number of water molecules around oxygen atoms depends on how exposed these oxygens are to the water, and therefore directly related to the position of these oxygen atoms along the EO chains, we divide all the oxygen atoms into three groups according to their distance from the aromatic core. The first group (inside atoms) include oxygen atoms bound directly to the core (atom numbers O, O1, O2, O3,

O4, O5 from the model given in the Figure 1B). The second group (middle atoms) includes oxygen atoms that are located in the middle of EO chains (atom numbers O6, O8, O10, O12, O16), and the final group (outside atoms) contains oxygen atoms that are those located at the end of EO chains (atom numbers O7, O9, O11, O13, O15, O17). The calculations were performed using the GROMACS tool trjorder.

The average numbers of water molecules around three different types of oxygen atom are given in Table III. The data presented includes values for a single TP6EO2M molecule in solution and an isolated dimer at 2 wt% to compare with the three values calculated from the self-assembly simulations.

Table III. Number of water molecules near oxygens atoms of EO chains for the two force fields and different TP6EO2M concentrations. The data for the three groups of oxygen atoms (inside, middle, and outside atoms) are given. See text for more details.

Number of TP6EO2M	inside oxygens		middle oxygens		outside oxygens	
	GAFF	OPLS	GAFF	OPLS	GAFF	OPLS
1	0.42±0.22	0.83±0.23	0.68±0.24	0.86±0.25	0.80±0.24	0.97±0.24
2 (2 wt %)		0.70±0.17		0.74±0.17		0.86±0.17
8 (8 wt %)	0.21±0.06	0.60±0.08	0.43±0.07	0.60±0.08	0.58±0.08	0.71±0.08
20 (8 wt %)	0.18±0.03	0.58±0.05	0.36±0.04	0.59±0.05	0.53±0.05	0.69±0.05
40 (16 wt %)	0.14±0.02	0.57±0.03	0.30±0.03	0.56±0.04	0.42±0.03	0.70±0.04

The obtained results for OPLS force field show three significant findings: (i) the amount of water around EO chains is smaller for molecules in stacks compared with a free molecule in solution and a dimer; (ii) the amount of water is (within error limits) the same for stacks of different lengths; (iii) the hydration of the outside oxygen atoms is stronger than that for inside and middle oxygens, while the hydration of the inside and middle oxygen atoms within the stacks is the nearly the same.

For a single TP6EO2M molecule in water (unaffected by the presence of the other molecules) we have obtained on average 0.97, 0.86 and 0.83 water molecules for outside, middle and inside oxygen groups respectively. As two molecules aggregate into a dimer, the number of water molecules decreases to 0.86, 0.74 and 0.70 for the same oxygen groups. The decrease in water amount is the largest for the inside oxygen atoms (~16 %) and the smallest for outside oxygen atoms (~11 %), indicating that water is depleted from the gap between the aromatic cores. Hence, oxygen atoms which are closer to the core are affected more upon aggregation than those on the periphery.

For the stack of 8 molecules the numbers of water molecules around the oxygen atoms decrease more, to 0.70 for the outside oxygen atoms and to 0.60 for the middle and inside ones. This is an expected result as there is less space for water around EO chains of the molecules inside the stack, therefore these chains are less hydrated. To reinforce this point, we calculated the amount of water molecules for the chains on the molecules at the edges of the stack (the first and the last molecule of an aggregate) and the obtained values are the same as those for the dimer (within error bars). It is surprising to find the same amount of water around the middle and inside oxygen atoms. Intuitively, one might expect a continuous gradient of increasing water association moving out from the core. Such an effect could originate from the fact that the molecules in the stack are slightly off-set. This allows partial hydration of the EO groups even within a stack.

Another interesting point is that we do not see any significant difference in the water amount for the larger stacks. The obtained values for the systems involved 20 and 40 molecules are the same for the outside oxygen atoms and, the same within error bars, for the middle and inside ones. These small differences originate from the fact that the more molecules there are in the system, the greater proportion of them are inside the stack and the contribution from the end molecules becomes smaller. When the stacks are formed and equilibrated, the hydration of the EO chains does not depend on the stack length, at least within the considered concentration range.

The values obtained for the amount of water around the oxygens in the GAFF force field are given for comparison. These are much lower than those obtained for the OPLS force field and the number of water molecules around oxygen atoms strongly decreases when the number or concentration of the chromonic molecules increases. Low amount of water around EO chains is a consequence of the stronger attractive interactions between the molecules and an insufficient attraction between EO groups and water within GAFF. As a result we obtained unrealistic compact aggregates upon self-assembly which have very limited space for water molecules inside them driven by a hydrophobic interaction.

To estimate the reliability of our results we compare them with the available experimental data for non-ionic $C_{12}EO_m$ surfactants and with the values obtained for PEO chains in water. The water activity measurements for non-ionic surfactants of $C_{12}EO_m$ type predict approximately one water molecule per EO group in lamellar phases and between one and two water molecules in a hexagonal phase.[52, 53] Considering that TP6EO2M stacks better resemble hexagonal micelles then lamellar, our result of 0.7 water molecules for terminal oxygens and 0.6 for the two others are thus lower than those found for $C_{12}EO_m$. However, we should note that in our chromonic molecules EO chains are rigidly connected to the aromatic core with limited ability to move and the radius of TP6EO2M molecules is much smaller than those for hexagonal micelles. That leads to much smaller area available for water around EO groups in TP6EO2M stacks. Also, the methyl group at the end of EO chains in the chromonic (O-CH3) is more hydrophobic than the hydroxyl (OH) group for the surfactants, further lowering hydration values. Taking into account each of these factors, our hydration values fall within the expected limits.

Calculations for a single polyethylene oxide (PEO) chain in water show that there is on average one (1.0 ± 0.1) water molecule in a shell of 0.3 nm around each oxygen atom. These calculations are also consistent with the number of EO-water hydrogen bonds for the same chain. This model was previously used to study properties of PEO chains.[28] The experimental values range between 0.5 and 6 water molecules per EO group, depending on the on the experimental technique applied,[54-58] with larger numbers associated with both direct and indirect (via water bridges) bound water.[54, 56, 59, 60]

3.5 Thermodynamic analysis

To gain insight into the driving force(s) for aggregation of the molecules, we performed thermodynamic analysis, separating entropic and enthalpic contribution of the free energy of association. Such analysis was performed previously in experimental work[16] for TP6EO2M molecules at low concentrations, using the data from NMR chemical shift experiments. To obtain the entropy and enthalpy components we have obtained the free energy of association of a molecule to a stack of three molecules for different temperatures in a range of 280-320 K. The entropy change in the system upon aggregation is calculated according to:

$$\Delta_{agg}G^0 = \Delta H - T\Delta S$$

$$\frac{\Delta_{agg}G^0}{RT} = \frac{\Delta H}{RT} - \frac{\Delta S}{R} \qquad (6)$$

$$R\left[\frac{\partial\left(\Delta_{agg}G^0/RT\right)}{\partial(1/T)}\right]_P = \Delta H$$

The slope $\dfrac{\partial\left(\Delta_{agg}G^0/RT\right)}{\partial(1/T)}$ was calculated by numerical differentiation of the $\dfrac{\Delta_{agg}G^0}{RT}\left(\dfrac{1}{T}\right)$ plot. The results for ΔH, $T\Delta S(T)$ and $\Delta_{agg}G^0(T)$ are given in Figure 6 together with experimental values adapted from ref. [16]. The experimental data were obtained for different chromonic mole fractions in the range of $4.8\times10^{-5} - 2.4\times10^{-4}$ (0.25 −1.24 wt %). In simulation, to achieve such a low concentration would require a prohibitive large number of water molecules, hence we adopted a higher concentration of 1.9 wt % or mole fraction 3.64×10^{-4}. To be consistent with the experiments we have extrapolated experimental data for $\Delta_{agg}G^0$ to the concentration similar to ours in simulations.
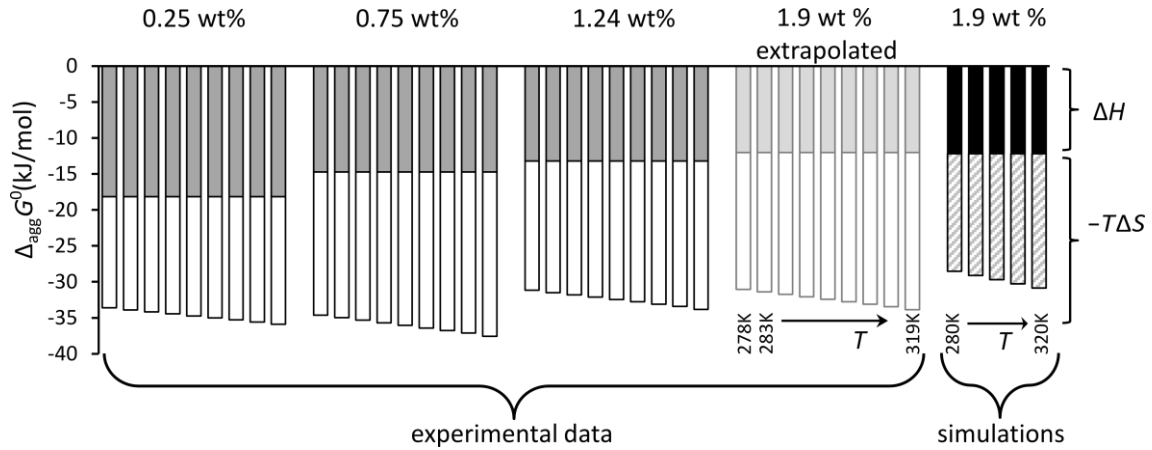
Figure 6. Free energy of association $\Delta_{agg}G^0(T)$ decomposed into ΔH and $T\Delta S(T)$ contributions. First three sets of data are for experimental results at different concentrations. The fourth set of data is obtained using extrapolated experimental results for $\Delta_{agg}G^0$. For experimental data ΔH is shown as grey and $T\Delta S(T)$ as white columns. The temperature in experiment was sampled in a range of 278 – 319 K with an increment of 5 K except for the last value of 319 K. The last set of data is our simulation results, where $\Delta_{agg}G^0$ is obtained using Wertheim approach applied to the PMF profiles for binding a molecule to a stack of three molecules. For simulation data ΔH is shown as black and $T\Delta S(T)$ as hatched columns. The temperature range in simulation was 280 – 320 K with an increment of 10 K.

The experimental calculations yield values for $\Delta_{agg}G^0(T)$ in a range of −31.9 to −36 kJ/mol (−13.1 to −14.5 RT) what result in extracted ΔH values in a range of −12 to −18 and $T\Delta S$ values in a range of 15–23 kJ/mol. In simulations we obtained ΔG values in a range of −28.8 to 30.1 kJ/mol (−11.6 to −12.4 RT). Decomposition of $\Delta_{agg}G^0(T)$ for enthalpic and entropic terms gives $\Delta H = −12.2$ kJ/mol and the entropic term $T\Delta S$ in a range of 16.3 – 18.7 kJ/mol. The errors for ΔH and $T\Delta S$ were estimated from the slope and intercept of the $\left(\Delta_{agg}G^0/RT\right)$ vs. $1/T$ plot and are about 1 kJ/mol for experimental

data and 3 kJ/mol for simulations results. We note that even a small difference in slope $\dfrac{\partial\left(\Delta G / RT\right)}{\partial\left(1/T\right)}$ strongly affects the values of ΔH and ΔS and therefore, taking into account considerably large errors we can only make qualitative not quantitative conclusions.

Both terms, entropic and enthalpic, are of the same order of magnitude and both favour the aggregation. However, except for the lowest concentration (0.25 wt%), both experimental and simulation results yield entropic contributions higher than the enthalpic ones. At the lowest experimental concentration (0.25 wt%) the entropic term is slightly higher (for 2-15 % depending on the temperature) than the entropic one, implying that at very low concentrations aggregation is energetically favourable. At the concentrations higher than 0.25 wt% the entropic term dominates by 20-90% (the higher the concentration, the higher $T\Delta S$ and the smaller ΔH). As for simulation results, the calculated values for the entropic contributions are 30-50 % higher than the enthalpic one. It is likely that it is the entropy change in the system that plays the key role in the molecular aggregation for TP6EO2M.

Conclusions

We have carried out atomistic simulations of the non-ionic chromonic molecule TP6EO2M in aqueous solution at low concentrations corresponding to the isotropic phase. The results obtained with two widely used force-fields, GAFF and OPLS, were analysed and compared.

Our results clearly demonstrated that OPLS force field works well for this type of molecules. We have obtained reasonable results for molecular self-assembly into stacks, aggregation free energy and intermolecular distance. The GAFF force field, which has been successfully used for other chromonics,[23, 61] treats the interactions between EO groups and water molecules poorly and this means the side-to-side interactions between TP6EO2M molecules are too favourable. This leads to reduced hydration of oxygens in EO side chains, too strong attraction between chromonic molecules and, as consequence, molecular aggregation into compact disorganized clusters instead of ordered stacks.

The OPLS force field provides useful insight into the hydration of EO groups. The hydration was examined for both, a single TP6EO2M molecule in water and for self-assembled stacks. The values obtained for a single molecule agree with the simulation and experimental data for PEO chains in water. For the molecules in the stack the hydration is found to be consistently lower than for a single molecule due to water depletion. However, taking into account molecular structure, they agree reasonably well with the experimental data for $C_{12}EO_m$ type surfactants. We also found the same hydration of the middle and inside oxygen atoms. This effect could be attributed to the fact that the molecules in the stack are slightly off-set allowing hydration of the EO groups within the stack.

We have found that the stacking distance between the molecule (d_S = 0.37 nm) lie at the top of the range usually cited for other (ionic) chromonics (0.33-0.37 nm). We believe that relatively large layer spacing originates from the steric repulsion of EO chains.

The calculations of binding free energy for OPLS force field show that the aggregation is nearly isodesmic except for the formation of dimers. The obtained value of free energy for the addition of a molecule to a stack ($\Delta_{agg}G^0$ = −12 RT) is reasonably close to the corresponding experimental value (~−14 RT) and in line with those reported for typical chromonics (−7 to −12 RT). The subsequent thermodynamic analysis shows that both the enthalpic and entropic components favour aggregation. The obtained values for $T\Delta S$ are up to 1.5 times larger than those for ΔH and allow us to suggest that the entropic contribution is the dominant term in the molecular aggregation.

References

1.   J. Lydon, *Current Opinion in Colloid & Interface Science*, 1998, **3**, 458-466.
2.   J. Lydon, *Current Opinion in Colloid & Interface Science*, 2004, **8**, 480-490.
3.   J. Lydon, *Journal of Materials Chemistry*, 2010, **20**, 10071-10099.
4.   J. Lydon, *Liquid Crystals*, 2011, **38**, 1663-1681.
5.   A. J. Dickinson, N. D. LaRacuente, C. B. McKitterick and P. J. Collings, *Molecular Crystals and Liquid Crystals*, 2009, **509**, 751-762.
6.   H.-S. Park, A. Agarwal, N. A. Kotov and O. D. Lavrentovich, *Langmuir*, 2008, **24**, 13833-13837.
7.   K. V. Kaznatcheev, P. Dudin, O. D. Lavrentovich and A. P. Hitchcock, *Physical Review E*, 2007, **76**.
8.   S. V. Shiyanovskii, O. D. Lavrentovich, T. Schneider, T. Ishikawa, Smalyukh, II, C. J. Woolverton, G. D. Niehaus and K. J. Doane, *Molecular Crystals and Liquid Crystals*, 2005, **434**, 587-598.
9.   S. V. Shiyanovskii, T. Schneider, Smalyukh, II, T. Ishikawa, G. D. Niehaus, K. J. Doane, C. J. Woolverton and O. D. Lavrentovich, *Physical Review E*, 2005, **71**.
10.   C. Rodriguez-Abreu, C. Aubery Torres and G. J. T. Tiddy, *Langmuir*, 2011, **27**, 3067-3073.
11.   N. Boden, R. J. Bushby and C. Hardy, *Journal De Physique Lettres*, 1985, **46**, L325-L328.
12.   N. Boden, R. J. Bushby, L. Ferris, C. Hardy and F. Sixl, *Liquid Crystals*, 1986, **1**, 109-125.
13.   N. Boden, R. J. Bushby, C. Hardy and F. Sixl, *Chemical Physics Letters*, 1986, **123**, 359-364.
14.   L. M. Ferris, PhD Thesis, The University of Leeds, 1989.
15.   S. D. Towlson, PhD Thesis, The University of Leeds, 1990
16.   J. F. Hubbard, PhD Thesis, The University of Leeds, 1997
17.   R. Hughes, A. Smith, R. Bushby, B. Movaghar and N. Boden, *Molecular Crystals and Liquid Crystals Science and Technology Section a-Molecular Crystals and Liquid Crystals*, 1999, **332**, 3057-3067.
18.   M. P. Taylor and J. Herzfeld, *Journal of Physics-Condensed Matter*, 1993, **5**, 2651-2678.
19.   R. Hentschke, P. J. B. Edwards, N. Boden and R. J. Bushby, *Macromolecular Symposia*, 1994, **81**, 361-367.
20.   R. G. Edwards, J. R. Henderson and R. L. Pinning, *Molecular Physics*, 1995, **86**, 567-598.
21.   T. Bast and R. Hentschke, *Journal of Physical Chemistry*, 1996, **100**, 12162-12171.
22.   P. Vanderschoot and M. E. Cates, *Europhys. Lett.*, 1994, **25**, 515-520.
23.   F. Chami and M. R. Wilson, *J Am Chem Soc*, 2010, **132**, 7794-7802.
24.   D. Van der Spoel, E. Lindahl, B. Hess, G. Groenhof, A. E. Mark and H. J. C. Berendsen, *J Comput Chem*, 2005, **26**, 1701-1718.
25.   B. Hess, C. Kutzner, D. van der Spoel and E. Lindahl, *J Chem Theory Comput*, 2008, **4**, 435-447.
26.   A. Minoia, L. P. Chen, D. Beljonne and R. Lazzaroni, *Polymer*, 2012, **53**, 5480-5490.
27.   A. Minoia, Chemibytes, http://chembytes.wikidot.com/grocnt#toc3
28.   S. Nawaz and P. Carbone, *Journal of Physical Chemistry B*, 2014, **118**, 1648-1659.
29.   M. Sedghi, L. Goual, W. Welch and J. Kubelka, *Journal of Physical Chemistry B*, 2013, **117**, 5765-5776.
30.   N. Boden, R. J. Bushby, K. W. Jolley, M. C. Holmes and F. Sixl, *Molecular Crystals and Liquid Crystals*, 1987, **152**, 37-55.
31.   B. Hess, *J Chem Theory Comput*, 2008, **4**, 116-122.
32.   W. G. Hoover, *Physical Review A*, 1985, **31**, 1695-1697.
33.   S. Nose, *Molecular Physics*, 1984, **52**, 255-268.
34.   S. Nose and M. L. Klein, *Molecular Physics*, 1983, **50**, 1055-1076.
35.   M. Parrinello and A. Rahman, *Journal of Applied Physics*, 1981, **52**, 7182-7190.
36.   T. Darden, D. York and L. Pedersen, *Journal of Chemical Physics*, 1993, **98**, 10089-10092.

37.   U. Essmann, L. Perera, M. L. Berkowitz, T. Darden, H. Lee and L. G. Pedersen, *Journal of Chemical Physics*, 1995, **103**, 8577-8593.

38.   W. Humphrey, A. Dalke and K. Schulten, *Journal of Molecular Graphics & Modelling*, 1996, **14**, 33-38.

39.   C. B. McKitterick, N. L. Erb-Satullo, N. D. LaRacuente, A. J. Dickinson and P. J. Collings, *Journal of Physical Chemistry B*, 2010, **114**, 1888-1896.

40.   G. J. T. Tiddy, D. L. Mateer, A. P. Ormerod, W. J. Harrison and D. J. Edwards, *Langmuir*, 1995, **11**, 390-393.

41.   A. Villa, C. Peter and N. F. A. van der Vegt, *Physical Chemistry Chemical Physics*, 2009, **11**, 2077-2086.

42.   A. Villa, N. F. A. van der Vegt and C. Peter, *Physical Chemistry Chemical Physics*, 2009, **11**, 2068-2076.

43.   C. Li, J. Shen, C. Peter and N. F. A. van der Vegt, *Macromolecules*, 2012, **45**, 2551-2561.

44.   M. S. Wertheim, *Journal of Statistical Physics*, 1984, **35**, 19-34.

45.   M. S. Wertheim, *Journal of Statistical Physics*, 1984, **35**, 35-47.

46.   M. S. Wertheim, *Journal of Statistical Physics*, 1986, **42**, 459-476.

47.   M. S. Wertheim, *Journal of Statistical Physics*, 1986, **42**, 477-492.

48.   J. D. Weeks, D. Chandler and H. C. Andersen, *Journal of Chemical Physics*, 1971, **54**, 5237-+.

49.   J.-P. Hansen and I. R. McDonald, *Theory of simple liquids*, Academic Press 3rd ed., Amsterdam, 2006.

50.   A. Thuresson, M. Ullner, T. Akesson, C. Labbez and B. Jonsson, *Langmuir*, 2013, **29**, 9216-9223.

51.   M. Walker, A. J. Masters and M. R. Wilson, *PCCP*, 2014.

52.   M. Carvell, D. G. Hall, I. G. Lyle and G. J. T. Tiddy, *Faraday Discussions*, 1986, **81**, 223-237.

53.   K. Rendall and G. J. T. Tiddy, *Journal of the Chemical Society-Faraday Transactions I*, 1984, **80**, 3339-3357.

54.   K. Sasahara, M. Sakurai and K. Nitta, *Colloid Polym. Sci.*, 1998, **276**, 643-647.

55.   S. Magazu, *Journal of Molecular Structure*, 2000, **523**, 47-59.

56.   E. E. Dormidontova, *Macromolecules*, 2002, **35**, 987-1001.

57.   K. J. Liu and J. L. Parsons, *Macromolecules*, 1969, **2**, 529-&.

58.   J. Maxfield and I. W. Shepherd, *Polymer*, 1975, **16**, 505-509.

59.   N. B. Graham, M. Zulfiqar, N. E. Nwachuku and A. Rashid, *Polymer*, 1989, **30**, 528-533.

60.   R. Kjellander and E. Florin, *Journal of the Chemical Society-Faraday Transactions I*, 1981, **77**, 2053-2077.

61.   F. Chami, M. R. Wilson and V. S. Oganesyan, *Soft Matter*, 2012, **8**, 6823-6833.